



MiR-377-3p suppresses colorectal cancer through negative regulation on Wnt/ β -catenin signaling by targeting XIAP and ZEB2

Lifeng Huang^{a,c,1}, Zhibo Liu^{b,c,1}, Jia Hu^{c,1}, Zhen Luo^c, Cheng Zhang^c, Lin Wang^{a,c,*}, Zheng Wang^{b,c,*}

^a Department of Clinical Laboratory, Union Hospital, Tongji Medical College, Huazhong University of Science and Technology, Wuhan, 430022, China

^b Department of Gastrointestinal Surgery, Union Hospital, Tongji Medical College, Huazhong University of Science and Technology, Wuhan, 430022, China

^c Research Center for Tissue Engineering and Regenerative Medicine, Union Hospital, Tongji Medical College, Huazhong University of Science and Technology, Wuhan, 430022, China

ARTICLE INFO

Keywords:

MiR-377-3p
 β -catenin
ZEB2
XIAP
Colorectal cancer

ABSTRACT

Aberrant activation of Wnt/ β -catenin signaling is a common event in the development of colorectal cancer (CRC). It is important to identify new molecules and mechanisms that can negatively regulate Wnt/ β -catenin signaling. MicroRNAs are considered as promising candidates for cancer diagnosis and therapy. In our study, we found that miR-377-3p was significantly decreased in CRC samples compared to the normal mucosa tissues, especially in the patients at stage III/IV. Functional studies showed that overexpression of miR-377-3p suppressed and silence of miR-377-3p enhanced the proliferation, migration and chemoresistance of CRC cells. Molecularly, miR-377-3p inhibited Wnt/ β -catenin signaling by directly targeting ZEB2 and XIAP, which were the positive regulators of Wnt/ β -catenin signaling. Overexpression of ZEB2/XIAP could counteract the tumor suppressing phenotypes induced by miR-377-3p. Therefore, we uncovered the anti-cancer role and the relevant mechanisms of miR-377-3p in CRC, which might provide novel targets for designing new anti-tumor strategies.

1. Introduction

Colorectal cancer (CRC) is the fourth most common cancer with high mortality rates in the world [1]. Although surgery and adjuvant chemo-radiotherapy provide effective treatment for CRC, a large number of patients still experience distant metastasis and tumor recurrence [2,3]. The 5-years survival rate of these patients is even lower than 10 % [4]. At present, the underlying mechanisms of CRC tumorigenesis and progression remain largely unclear. This promotes us to find key molecules and mechanisms that may contribute to the highly malignant phenotypes and identify novel effective therapeutic targets.

Wnt/ β -catenin signaling is a highly conserved pathway that controls numerous biological and pathological processes, such as embryonic development and tumorigenesis [5,6]. It is frequently deregulated (80 %–90 %) and considered as a potential therapeutic target in CRC [7,8]. β -catenin, the key molecule of canonical-Wnt cascade, is regulated by a complex containing glycogen synthase kinase 3 β (GSK3 β),

adenomatous polyposis coli (APC) and AXIN. In the absence of Wnt ligands, β -catenin is phosphorylated by the destruction complex and targeted for degradation [9]. Once Wnt signaling is activated, β -catenin translocates to the nucleus and works with the T-cell factor/lymphoid enhancer factor (TCF/LEF) family to regulate transcription of downstream genes [10]. Dysregulation of Wnt/ β -catenin signaling is a critical driver in CRC development and metastasis. Multiple molecules were reportedly involved in Wnt/ β -catenin signaling regulation, such as microRNAs (miRNAs) [11–13].

MiRNAs are a class of small non-coding RNAs that negatively regulate the target genes by binding to 3'untranslated region of target genes [14]. Numerous studies indicated that miRNAs were implicated in tumor development [15,16]. MiR-377 has drawn interests as it acts as a tumor suppressor in many types of cancers [17–20]. For example, miR-377 inhibited initiation and progression of esophageal cancer by targeting CD133 and VEGF [18]. In gastric cancer, miR-377 suppressed cell proliferation and metastasis via repressing VEGFA expression [20].

Abbreviations: CRC, colorectal cancer; GSK3 β , glycogen synthase kinase; TCF/LEF, T-cell factor/lymphoid enhancer factor; APC, adenomatous polyposis coli; XIAP, X-linked inhibitor of apoptosis protein; ZEB2, Zinc Finger E-Box Binding Homeobox 2; pre-miRNAs, precursor-microRNAs

* Corresponding authors at: Research Center for Tissue Engineering and Regenerative Medicine, Union Hospital, Tongji Medical College, Huazhong University of Science and Technology, Wuhan, 430022, China.

E-mail addresses: lin_wang@hust.edu.cn (L. Wang), zhengwang@hust.edu.cn (Z. Wang).

¹ These authors contributed equally to this work.

<https://doi.org/10.1016/j.yphrs.2020.104774>

Received 20 August 2019; Received in revised form 16 February 2020; Accepted 22 March 2020

Available online 24 March 2020

1043-6618/ © 2020 Published by Elsevier Ltd.

However, the functions and relevant mechanisms of miR-377 in CRC remain unclear.

Here, we found that miR-377-3p was significantly downregulated in CRC. *In vitro* and *in vivo* results demonstrate that miR-377-3p suppresses the proliferation, migration and chemoresistance of CRC. This was mechanistically because miR-377-3p directly targeted XIAP (X-linked inhibitor of apoptosis protein) and ZEB2 (Zinc Finger E-Box Binding Homeobox 2) to negatively regulate Wnt/ β -catenin signaling. Our study suggests that miR-377-3p may serve as a potential therapeutic target for CRC.

2. Materials and methods

2.1. Antibodies and reagents

The antibodies used in this study were as follows: Vimentin (CST, cat.5741), N-cadherin (CST, cat.13116), E-cadherin (CST, cat.3195), β -catenin (Protein tech, cat.51067-2-AP), CyclinD1 (Boster, cat.BA0770), XIAP (Abclonal, A6869), ZEB2 (Santa Cruz Tech, cat.sc48789), C-Myc (Santa Cruz Tech, cat.sc-40), Axin2 (Affinity, DF-08670), MMP9 (CST, cat.13667), MMP2 (CST, cat.13132). 5-FU (5-Fluoracil) was purchased from Medchemexpress LLC (Monmouth Junction, NJ, USA).

2.2. Cell culture and transfection

293 T and human colorectal cancer cell lines LoVo, SW48 were obtained from ATCC (American Type Culture Collection, Manassas, VA). All cells were cultured in DMEM medium (Hyclone, Logan, UT) supplemented with 10 % fetal bovine serum (ScienCell, Carlsbad, CA) and maintained in a cell incubator with 5 % CO₂ at 37 °C. Cells were transfected using Lipofectamine 2000 (Invitrogen) according to the manufacturer's instructions and then processed as described for each experiment.

2.3. Small interfering RNAs and MicroRNA mimics

Small interfering RNAs (siRNAs) targeting β -catenin (si β -catenin), non-targeting siRNA negative control (siNC), miR-377-3p inhibitor, non-targeting miRNA inhibitor negative control (miRNA inhibitor NC), miR-377-3p mimics and miRNA negative control (miRNA NC) were purchased from GenePharma (Suzhou, China). The siRNA sequence information was showed in Table S1. All these siRNAs and miRNAs were transfected into CRC cells using Lipofectamine 2000 according to the manufacturer's instructions.

2.4. Plasmids construction, lentiviral transduction

The 3'-UTR of ZEB2 and XIAP were amplified from cDNA and ligated into the luciferase reporter plasmid pCMV-Tag2B-Luc at the restriction sites of EcoRI and Sall to generate pCMV-Luc-ZEB2-3'UTR and pCMV-Luc-XIAP-3'UTR. **The pMIR-miR-377-3p-GFP plasmid was purchased from Vigene Biosciences (Shandong, China). Pri-miR-377-3p was amplified from the pMIR-miR-377-3p-GFP plasmid and inserted into the pLenti-puro-3XFlag lentivirus vector to generate pLenti-3XFlag-miR-377-3p.** ShRNAs targeting XIAP and ZEB2 were cloned into the pLKO.1-TRC plasmid (Addgene plasmid # 10878).

For virus packaging, envelope plasmid pMD2.G (Addgene plasmid #12259), packaging plasmid psPAX2 (Addgene plasmid #12260) and expression pLenti-vectors (pLenti-puro-3XFlag, pLenti-puro-miR-377-3p, pLKO.1-shNC, pLKO.1-shZEB2 and pLKO.1-shXIAP) were co-transfected into HEK293 T cells. Medium was replaced with DMEM after 6 h. The virus supernatant was collected at 48 h after medium replacement. For virus transduction, CRC cells were infected with virus supernatant with **8 μ g/mL Polybrene** (Sigma-Aldrich) overnight, then the medium was replaced with fresh medium. The cells were selected by **puromycin (Biosharp) for 2 weeks.**

2.5. Western blot

Cells were washed with PBS before harvest and total protein was collected using the RIPA lysis buffer (Beyotime Institute of Biotechnology). Protein concentration was measured by the BCA protein assay reagent. Cell lysates were separated by SDS-polyacrylamide gel electrophoresis (SDS-PAGE) and then transferred to nitrocellulose membranes (Bio-Rad, Richmond, CA). The signal was visualized using a chemiluminescence system (UVP, San Gabriel, CA). GAPDH was used as control.

2.6. Reverse transcription reaction and quantitative real time PCR

Total RNA was extracted by Trizol (Takara Shuzo Co. Ltd, Kyoto, Japan) according to the manufacturer's recommendation. Synthesis of complementary DNA (cDNA) was performed using M-MLV reverse transcriptase (Thermo Scientific, Hudson, NH). Reverse transcriptase reactions of miRNAs were performed using a Stem-loop miRNA qRT-PCR Primer Sets. The quantitative RT-PCR was performed using the SYBR Green PCR kit (Takara Shuzo Co. Ltd, Kyoto, Japan) with the Real-Time PCR system (Applied Biosystems7500, Foster City, CA). The expression levels of mRNA and miRNA were calculated using the 2^{- $\Delta\Delta$ Ct} method with GAPDH or U6 snRNA as endogenous control. Sequences of primers used in the study were listed in Table S2.

2.7. Luciferase reporter assay

For luciferase activity analysis, HEK293 T cells were seeded and transfected with indicated plasmids. Luciferase activities were detected by the Dual Luciferase Assay Kit (Promega, Madison, WI) according to the manufacturer's instructions. Firefly luciferase activities were normalized by Renilla luciferase activities.

2.8. Proliferation assay and cell cytotoxicity assay

For the cell growth curve detection, 1000 cells per well were seeded in 96-well plate. Cell viability was tested every day by CCK-8 assay kit (Dojindo, Japan) according to the manufacturer's instructions. For Cell cytotoxicity assay, 5000 cells per well were cultured in 96-well plate with DMEM containing 10 % FBS. After 24 h incubation, it was replaced by DMEM containing indicated concentrations 5-FU. CCK-8 assay kit was used to detect cell viability after 48 h.

2.9. Tumor cell migration assay

Cells were cultured in 6-well plate until grew into the density of 80 % confluent. Then cells were suspended with serum-free DMEM and adjusted to a density of 5 \times 10⁴ /200 μ l. 200 μ l suspended cells were added into the upper chamber of the transwell device (Corning Inc, Acton, MA). The lower chamber was filled with 500 μ l DMEM supplemented with 10 % FBS. After 12 h (SW48 cells) or 24 h (LoVo cells), cells were fixed by 4 % paraformaldehyde and stained with crystal violet. The representative images were taken by microscope.

2.10. Focus colony formation assay and Soft agar colony formation assay

For focus colony formation assay, cells were seeded in 6-well plates at a density of 1000 cells per well and incubated with DMEM supplemented with 10 % FBS. Two weeks later, colonies were fixed by 4 % paraformaldehyde and stained by 0.1 % crystal violet.

For soft agar colony formation assay, 1.6 % sterilized soft agar was warmed in incubator prior to use. 6 mL 37 °C preheated DMEM containing 10 % FBS was mixed with 6 mL 1.6 % soft agar. Then the mixed medium was added in the 6-well plate to make bottom layer. The 6-well plate was placed in the 4 °C refrigerator to allow agar mixture to solidify. 6000 indicated cells were suspended with 3 mL soft agar and 9 mL

preheated medium. Then added 1.5 mL cell mixture in the 6-well plate carefully to avoid deposition of any air bubbles into the plate well. The 6-well plate was plated in 4 °C refrigerator to allow agar mixture to solidify for 30 min. 4 weeks later, colonies were stained by 0.05 % crystal violet.

2.11. Xenograft tumor model

Animal studies were performed using 6-week-old BALB/c athymic nude mice. Mice were maintained in laminar flow rooms with constant temperature and humidity. The mice were anesthetized with pentobarbital sodium. LoVo cells (Vector control and miR-377-3p) were suspended with serum-free RPMI 1640 and adjusted to a density of 1×10^7 cells/mL. 100 μ L indicated cells were subcutaneously inoculated into each flank of the mice. 5 days post injection, the tumor size was measured every other day. The tumor size was calculated using the formula: $V = (\text{length} \times \text{width}^2)/2$. 25 days after injection, the mice were euthanized and the tumors and livers were isolated. For survival curve, tumor-loaded mice were checked every 2 or 3 days. In addition, once the first mouse died, mice were checked every day.

For post-implantation therapeutic experiments, 1×10^6 LoVo cells were subcutaneously inoculated into each flank of the nude mice ($n = 5$ per group). Once the tumors reached 0.5 cm³, the mice were randomized to receive the treatments of PBS, miR-377-3p agomir (75 mg/kg) or NC agomir (75 mg/kg) every 3 days for consecutive 6 times. Eighteen days after the treatment, the mice were euthanized and the tumors were isolated.

2.12. Statistical analysis

Results were performed with GraphPad Prism 5 and presented as the means \pm standard deviation (SD). Survival curves were analyzed using the Kaplan-Meier method and assessed according to the log rank test. Other comparisons were analyzed by using Student's t-test or One-way ANOVA. Statistical significance in this study was set at $P < 0.05$.

3. Results

3.1. MiR-377-3p is downregulated in CRC

Mature microRNAs are derived from pre-miRNAs (precursor-microRNAs) that are processed by Dicer and Drosha, producing a -3p or -5p suffix in opposite arms of the same denoted pre-miRNA [21]. To determine the main existing form of miR-377 in CRC, we analyzed the expression of mature miR-377 in CRC samples from TCGA. The expression of miR-377-3p was markedly higher than miR-377-5p, suggesting that miR-377-3p is the dominant form in CRC (Fig. 1A). By analyzing miR-377-3p expression in CRC tissues and normal colon mucosa tissues from the database GSE18392 and GSE48267, we found that miR-377-3p was significantly downregulated in CRC tissues (Fig. 1B). Moreover, both mRNA and serum levels of miR-377-3p were lower in the patients at the advanced stages (stage III/IV) (Fig. 1C, E). In GSE53159 that contains liver metastasis information, the serum levels of miR-377-3p in CRC patients with liver metastasis were lower than the patients without liver metastasis (Fig. 1D). The ROC curve analyses in GSE53159 showed that miR-377-3p could serve as a potential marker to differentiate stage IV CRC patients from stage I with AUC (ROC curve area) of 0.76, more effective than miR-21 and miR-203, which reportedly acted as the diagnostic biomarkers in CRC [22,23] (Fig. 1F). Therefore, these data reveal that miR-377-3p is downregulated and may act as an inhibitory factor in CRC progression.

3.2. MiR-377-3p suppresses cell migration, proliferation and chemoresistance in CRC

To verify the function of miR-377-3p in CRC, we transfected miR-

377-3p mimics or miR-377-3p inhibitor into SW48 and LoVo cells. Transwell assays showed that the cell migration ability was decreased in miR-377-3p overexpressing cells and increased in miR-377-3p silenced cells (Fig. 2A–D). EMT related proteins and MMPs play important roles in tumor metastasis. MiR-377-3p downregulated the expression of mesenchymal markers (ZEB2, Vimentin and N-cadherin) and MMPs (MMP2 and MMP9) while upregulated epithelial markers (E-cadherin) (Fig. 2E). The effects of miR-377-3p on Vimentin and E-cadherin were also confirmed by immunofluorescence (Fig. S1A, B).

We also explored other biological functions of miR-377-3p in CRC and found that overexpression of miR-377-3p slightly suppressed colony formation, proliferation and 5-FU resistance of CRC cells (Figs. 2F, H and S2A, C). Conversely, knockdown of miR-377-3p enhanced colony formation, proliferation and 5-FU resistance of CRC cells (Figs. 2G, H and S2B, D). Bcl2 (negative regulator) and Bax (positive regulator) are well known apoptosis related genes. MiR-377-3p could upregulate the expression of Bax and downregulate Bcl2 (Fig. 2I). Collectively, we demonstrate that miR-377-3p suppresses cell migration, proliferation and chemoresistance in CRC.

3.3. MiR-377-3p inhibits Wnt/ β -catenin signaling

Wnt/ β -catenin signaling plays an important role in CRC tumorigenesis and progression. We wondered whether miR-377-3p could modulate Wnt/ β -catenin signaling in CRC. The protein levels of β -catenin as well as its downstream effectors Axin2 and CyclinD1 were significantly decreased in miR-377-3p overexpressing cells and increased in miR-377-3p silenced cells (Fig. 3A). Similarly, we observed that miR-377-3p reduced β -catenin protein levels by immunofluorescence (Fig. 3B). Moreover, qRT-PCR showed that miR-377-3p negatively regulated the expression of Wnt/ β -catenin related genes including Cyclin D1, Axin2, TCF1, SOX2, C-myc, MMP2, MMP9, CD44, VEGF and Twist (Fig. 3C). To assess the effect of miR-377-3p on β -catenin activity, Wnt/ β -catenin signaling activator LiCl was used to treat miR-377-3p transfected cells. MiR-377-3p reduced β -catenin's transcriptional activity and protein levels at both the quiescent or activated states of Wnt/ β -catenin signaling (Fig. 3D). Then we determined whether Wnt/ β -catenin signaling was involved in miR-377-3p regulated cell migration. Wnt/ β -catenin signaling inhibitor XAV-939 abolished the migration promoted by miR-377-3p inhibitor in SW48 and LoVo cells (Fig. 3E, F). These findings suggest that miR-377-3p suppresses CRC through inhibiting Wnt/ β -catenin signaling.

3.4. MiR-377-3p directly targets the 3'UTR of ZEB2 and XIAP

MiR-377-3p failed to match with the 3'UTR of β -catenin, suggesting that miR-377-3p regulates Wnt/ β -catenin signaling through other target genes. To identify these genes, we screened the genes that contained miR-377-3p binding site in 3'UTR (from Targetscan website) and positively regulated β -catenin. Bioinformatics analysis revealed three putative candidate genes: ZEB2, XIAP and SOX11 (Fig. 4A). TCGA database analysis indicates that miR-377-3p is negatively correlated with ZEB2 and XIAP in CRC (Fig. 4B). To determine whether miR-377-3p regulated ZEB2 and XIAP by directly targeting their 3'UTR, ZEB2 and XIAP 3'UTR were constructed into a luciferase reporter plasmid (Fig. 4C). The luciferase activity of ZEB2 and XIAP 3'UTR was repressed by miR-377-3p in a dose-dependent manner (Fig. 4D, E). Mutations in either ZEB2/XIAP-3'UTR at the predicted matching sites or in miR-377-3p at the conserved binding site disrupted this repression (Fig. 4F, G). Both mRNA and protein levels of ZEB2 and XIAP were significantly decreased in miR-377-3p overexpressing cells and increased in miR-377-3p silenced cells in a dose-dependent manner (Fig. 4H). Taken together, these results suggest that ZEB2 and XIAP are the direct target genes of miR-377-3p.

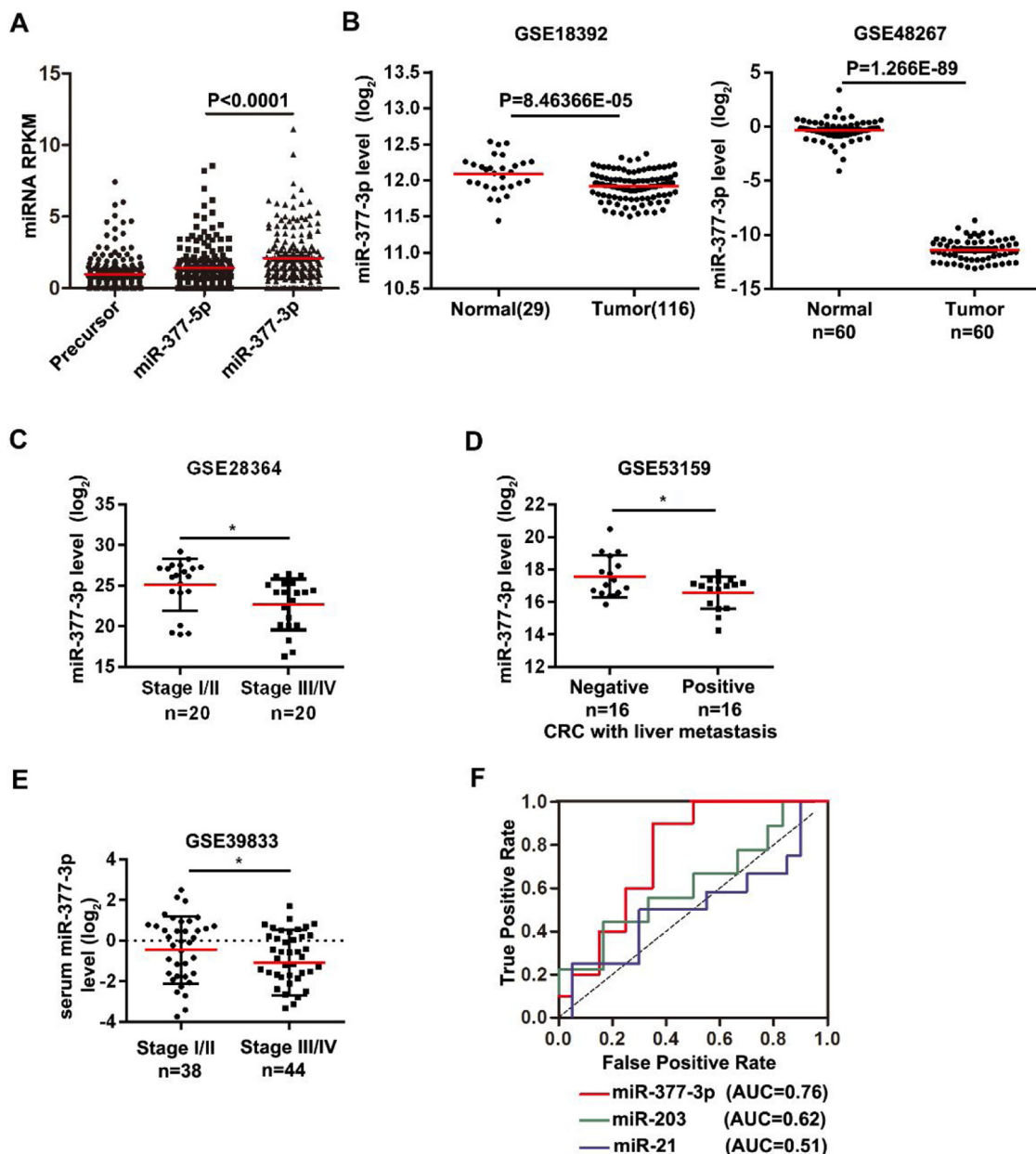


Fig. 1. Expression levels of miR-377-3p in CRC. (A) Analysis of different forms of mature miR-377-3p levels in 186 colon cancer samples from TCGA. (B) Analysis of miR-377-3p expression in colon cancer samples and normal colon mucosa tissues from GSE18392 (unpaired tissues) and GSE48267 (paired tissues). (C) Analysis of miR-377-3p mRNA expression in CRC samples at different tumor stages from GSE28364; *, $P < 0.05$. (D) Analysis of serum miR-377-3p levels in CRC samples with or without liver metastasis from GSE53159; *, $P < 0.05$. (E) Analysis of serum miR-377-3p levels in CRC patients at different tumor stages from GSE39833; *, $P < 0.05$. (F) Serum miR-377-3p predicted liver metastasis in 10 stage I and 10 stage IV patients from GSE53159. AUC represents area under the curve.

3.5. MiR-377-3p inhibits cell migration through targeting ZEB2 in CRC

ZEB2 reportedly upregulates β -catenin in glioma [24]. Meanwhile, ZEB2 is an EMT related transcriptional factor that plays an important role in cell migration and invasion [25]. We sought to determine whether ZEB2 was involved in miR-377-3p's modulation on Wnt/ β -catenin signaling and cell migration. We established ZEB2 stably knockdown cell line and found that knockdown of ZEB2 could down-regulate Vimentin and CyclinD1 (Fig. 5A). Moreover, knockdown of ZEB2 inhibited the upregulation of β -catenin and its downstream effectors including Cyclin D1, Axin2, TCF1, SOX2, C-myc, MMP2, MMP9, CD44, VEGF and Twist in miR-377-3p silenced cells (Fig. 5B, D). TOP-flash luciferase assays showed that the promoting effect of miR-377-3p inhibitor on Wnt/ β -catenin signaling was abrogated when ZEB2 was silenced (Fig. 5C). The upregulation of Vimentin and MMP2, and the

enhanced migration phenotype in miR-377-3p silenced cells were also abolished when ZEB2 was knockdown (Fig. 5D–F). Overexpression of ZEB2 rescued the dampened migration ability in miR-377-3p over-expressing cells (Fig. S4C). These results demonstrate that miR-377-3p represses CRC cells migration and Wnt/ β -catenin signaling by targeting ZEB2.

3.6. MiR-377-3p suppresses CRC cell proliferation and chemoresistance by targeting XIAP

XIAP was reported to monoubiquitylate Gro/TLE to enhance β -catenin transcriptional activity [26]. As another target gene of miR-377-3p, knockdown of XIAP also abrogated the promoting effect of miR-377-3p inhibitor on Wnt/ β -catenin signaling (Fig. 6A–C). XIAP is a member of inhibitor of apoptosis family proteins (IAP) that can promote

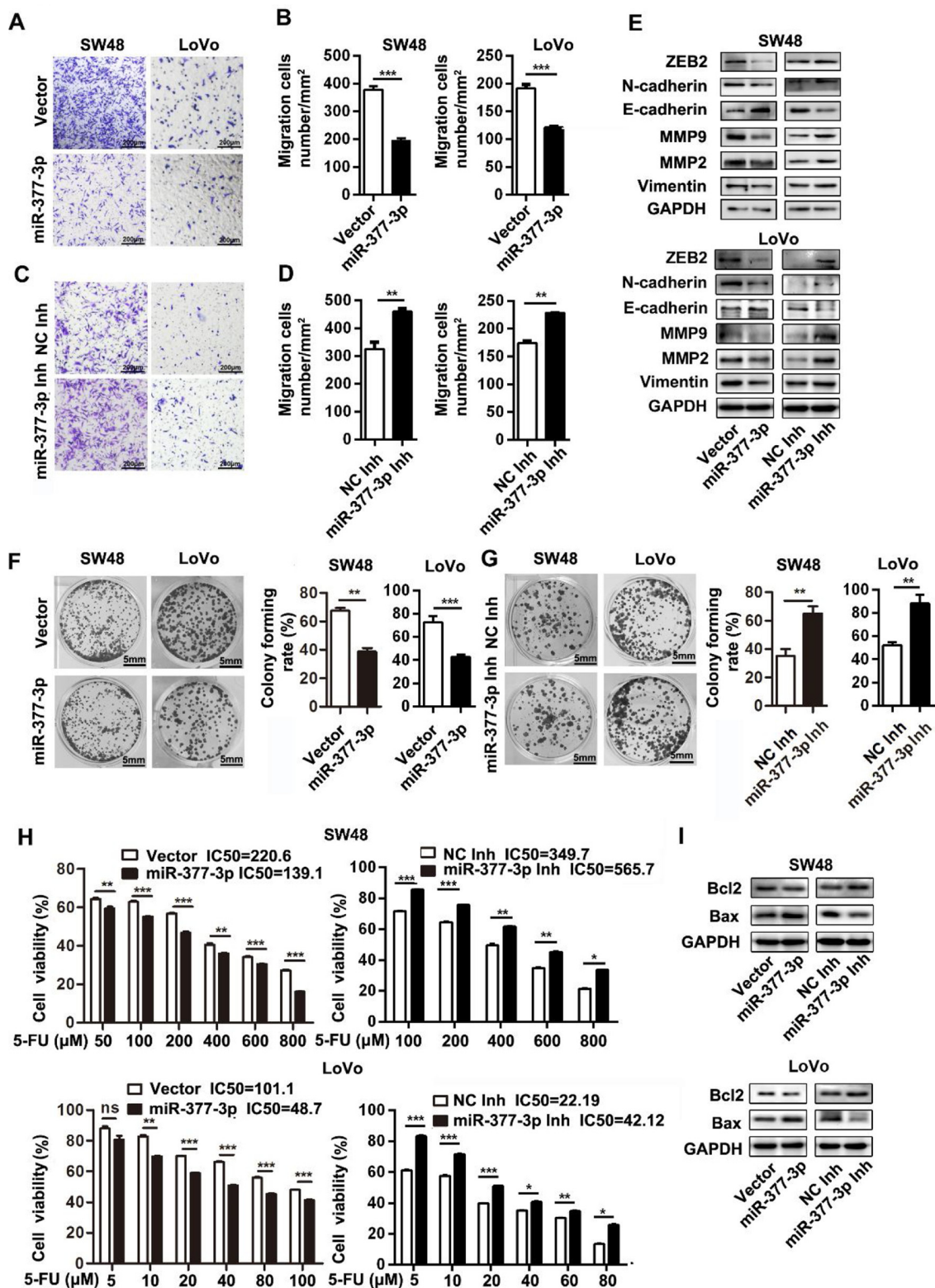
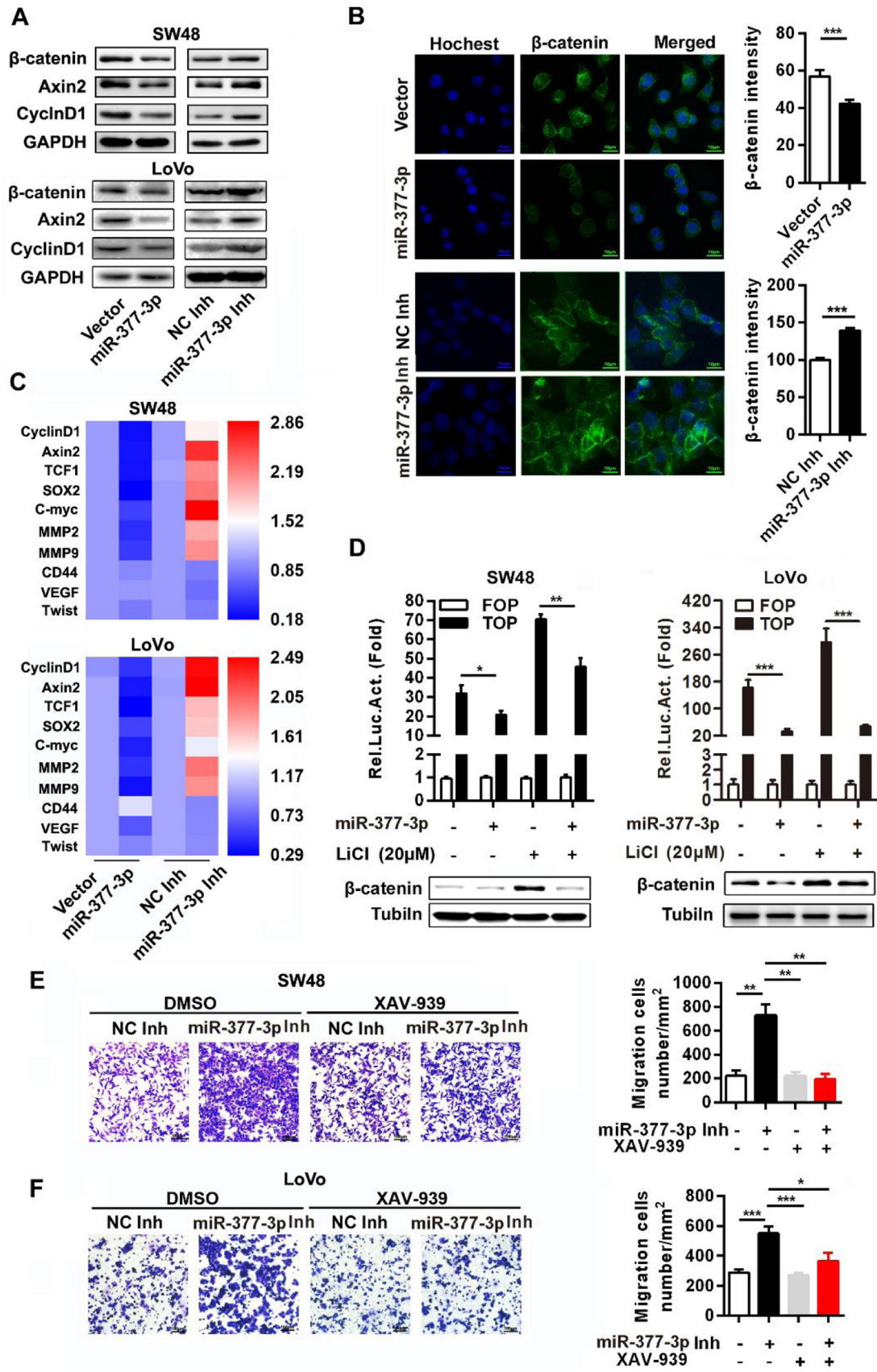


Fig. 2. MiR-377-3p suppresses cell migration, proliferation and chemoresistance in CRC. (A-D) Migration assays of SW48 or LoVo cells transfected with miR-377-3p mimics (A) or miR-377-3p inhibitor (C). Representative images were shown and the average number of cells per field were calculated (B, D). n = 3 samples per group, four fields per sample; Scale bars, 200 μm; **, P < 0.01; ***, P < 0.001. (E) SW48 or LoVo cells were transfected with miR-377-3p mimics or miR-377-3p inhibitor for 48 h. EMT markers (ZEB2, N-cadherin, E-cadherin, Vimentin) and MMPs (MMP9, MMP2) were detected by western blot. (F and G) Colony formation assays of SW48 or LoVo cells stably transfected with miR-377-3p plasmid (F) or transfected with miR-377-3p inhibitor (G). Colony numbers were calculated by ImageJ pro-plus. n = 3 samples per group; Scale bars, 5 mm; **, P < 0.01; ***, P < 0.001. (H) 5-FU cytotoxicity assays of SW48 or LoVo cells transfected with miR-377-3p inhibitor or stably overexpressing miR-377-3p. Cell viability was determined by CCK8 assay kits after being treated with indicated concentrations of 5-FU for 48 h. n = 3 samples per group; *, P < 0.05; **, P < 0.01; ***, P < 0.001. (I) SW48 or LoVo cells were transfected with miR-377-3p mimics or miR-377-3p inhibitor for 48 h. Bcl2 and Bax were detected by western blot.



(caption on next page)

Fig. 3. MiR-377-3p is a negative regulator of Wnt signaling. (A) SW48 or LoVo cells were transfected with miR-377-3p mimics or miR-377-3p inhibitor for 48 h. β -catenin, Axin2 and CyclinD1 were detected by western blot. (B) LoVo cells were transfected with miR-377-3p inhibitor for 24 h. Cells were fixed and immunofluorescently stained for β -catenin. Representative images were shown and the fluorescence intensity was calculated. Scale bars, 10 μ m; ***, $P < 0.001$. (C) SW48 and LoVo cells were transfected with miR-377-3p mimics or miR-377-3p inhibitor for 48 h. The downstream genes of Wnt signaling were detected by qPCR. The heatmap showed the changes in mRNA expression for the downstream genes of Wnt signaling. (D) SW48 or LoVo cells were co-transfected with miR-377-3p mimic (0.4 μ g) and TOP/FOP-flash reporter (0.1 μ g) for 24 h. Then cells were treated with or without 20 μ M LiCl for 12 h. Luciferase activity was measured and normalized to Rellina luciferase activity. $n = 3$ samples per group; *, $P < 0.05$; **, $P < 0.01$; ***, $P < 0.001$. β -catenin was detected by western blot. (E and F) SW48 (E) or LoVo (F) cells were transfected with miR-377-3p inhibitor for 24 h. Then cells were treated with or without XAV939 for 12 h and harvested for migration assays. Representative images were shown and the average number of cells per field were calculated. $n = 3$ samples per group, four fields per sample; Scale bars, 100 μ m; *, $P < 0.05$; **, $P < 0.01$; ***, $P < 0.001$.

cell growth and suppress apoptosis in CRC [27]. XIAP knockdown abolished the enhancement in colony formation (Figs. 6D, E and S3A, B), chemoresistance (Fig. 6F) and proliferation (Fig. 6G) in miR-377-3p silenced cells. In line with this, overexpression of XIAP restored the suppressed colony formation and chemoresistance in miR-377-3p stably overexpressing cells (Fig. S4A, B). Therefore, miR-377-3p suppresses the proliferation and chemoresistance of CRC cells via targeting XIAP.

3.7. MiR-377-3p inhibits CRC tumorigenesis and metastasis in vivo

To further explore the effects of miR-377-3p on CRC *in vivo*, nude mice were subcutaneously injected with LoVo cells stably expressing miR-377-3p. Overexpression of miR-377-3p repressed tumor growth (Fig. 7A, B), increased survival rate (Fig. 7C) and decreased the number of liver metastatic foci in mice (Fig. 7D–F). Immunohistochemical staining showed that the expression of Ki67, a cell proliferation marker, was significantly lower in miR-377-3p overexpression group (Fig. 7G). As the target genes of miR-377-3p, ZEB2 and XIAP were downregulated (Fig. 7G). Overexpression of miR-377-3p decreased the mesenchymal marker Vimentin and upregulated the epithelial marker E-cadherin (Fig. 7G). To assess the therapeutic potential of targeting miR-377-3p in established tumors, we subcutaneously injected LoVo cells into nude mice. After the tumors reached 0.5 cm³, we performed intra-tumoral injections of miR-377-3p agomir. Strikingly, injection of miR-377-3p agomir but not the control effectively inhibited tumor growth (Fig. 7H, I) and extended survival time of the mice (Fig. 7J). These data indicate that miR-377-3p represses CRC development and metastasis *in vivo*.

4. Discussion and conclusion

Aberrant expression of miRNAs is implicated in tumorigenesis and cancer progression [28]. MiR-377 was previously reported to act as a tumor suppressor in many types of cancers [18,19,29–31]. However, the functional roles and mechanisms of miR-377 in CRC remain unclear. Recently, a study reported that miR-377 could promote the malignant characteristics of CRC cells via targeting and upregulating GSK-3 β [32]. Contrary to their findings, our study showed that miR-377-3p could suppress the malignant phenotypes of CRC, including proliferative, invasive and drug resistant capabilities. This was supported by publically available clinical databases showing that miR-377-3p was significantly downregulated in CRC tissues, especially in patients at advanced stages. Compared to the previous study reporting that miR-377 promoted CRC progression, the functional experiments of miR-377-3p in our study were more reliable, particularly *in vivo* experiments. We had 15 mice in each group and performed the survival experiment of mice. More importantly, we conducted miRNA therapeutic experiment in the mouse xenografted cancer model, and found that miR-377-3p suppressed CRC growth *in vivo*. Therefore, our data strongly supports that miR-377-3p acts as a tumor suppressor in CRC.

Abnormal activation of Wnt/ β -catenin signaling is common in CRC [34]. Many studies have devoted to finding molecular targets that can inhibit Wnt/ β -catenin signaling to treat CRC [35,36]. MiRNAs have been considered as powerful therapeutic tools because of their small size and ability to repress the expression of multiple oncogenic targets [37]. We found that miR-377-3p negatively regulated the Wnt/ β -

catenin signaling cascade by targeting the 3'UTR of two positive regulators of Wnt/ β -catenin signaling, ZEB2 and XIAP. We also provided evidences showing that miR-377-3p suppressed the progression of CRC via inhibiting Wnt/ β -catenin signaling, suggesting that miR-377-3p might be a potential therapeutic target for CRC treatment.

ZEB2 reportedly contribute to the loss of epithelial marker E-cadherin and upregulation of mesenchymal markers, including N-cadherin and Vimentin to facilitate tumor cell invasion in CRC [38,39]. ZEB2 was reported to promote the expression of β -catenin, suggesting ZEB2's positive regulatory role in Wnt/ β -catenin signaling [24]. Consistent with this notion, our study showed that knockdown of ZEB2 abrogated the promoting effect of miR-377-3p inhibitor on Wnt/ β -catenin signaling and cell migration in CRC, indicating that miR-377-3p's effects on Wnt/ β -catenin signaling relies on targeting ZEB2. Another miR-377-3p target gene was found to be XIAP, a member of inhibitor of apoptosis proteins (IAPs). Overexpression of XIAP was associated with poor prognosis and drug resistance in CRC [27,40]. XIAP could mono-ubiquitylate Groucho/TLE to promote canonical Wnt signaling, suggesting a link between apoptosis and Wnt/ β -catenin signaling [26]. Our work reveals that XIAP mediates miR-377-3p's regulation on Wnt/ β -catenin signaling, cell proliferation and chemoresistance in CRC. Thus, ZEB2 and XIAP are responsible for the miR-377-3p suppressed Wnt/ β -catenin signaling and CRC development.

In summary, our findings demonstrate that miR-377-3p can suppress the development of CRC, which is achieved by negatively regulating Wnt/ β -catenin signaling through targeting XIAP and ZEB2. This novel miR-377-3p/ZEB2-XIAP/Wnt axis provides a new insight into the mechanisms of CRC progression and may lead to the development of new anti-CRC therapies.

Author contributions

Conceptualization, L.-W. and Z.-W.; performed experiments and analyzed data, L.-F.H., Z.-B.L., J.-H., C.-Z., L.-W., and Z.-W.; data analysis and technique assistance, Z.-L.; data curation, Z.-B.L., J.-H.; paper writing, J.-H., Z.-L., and Z.-W.; supervision, L.-W. and Z.-W. All authors read and approved the final manuscript.

Declaration of Competing Interest

The authors declare no conflict of interests.

Acknowledgements

This work is supported by the Major State Basic Research Development Program of China (973 Program, 2015CB554007); the National Natural Science Foundation of China Programs (81572866, 81671904, 81773263, 81773104 and 31701202); the International Science and Technology Corporation Program of Chinese Ministry of Science and Technology (2014DFA32920); the Science and Technology Program of Chinese Ministry of Education (113044A); the Frontier Exploration Program of Huazhong University of Science and Technology (2015TS153); the Natural Science Foundation Program of Hubei Province (2015CFA049); the Integrated Innovative Team for

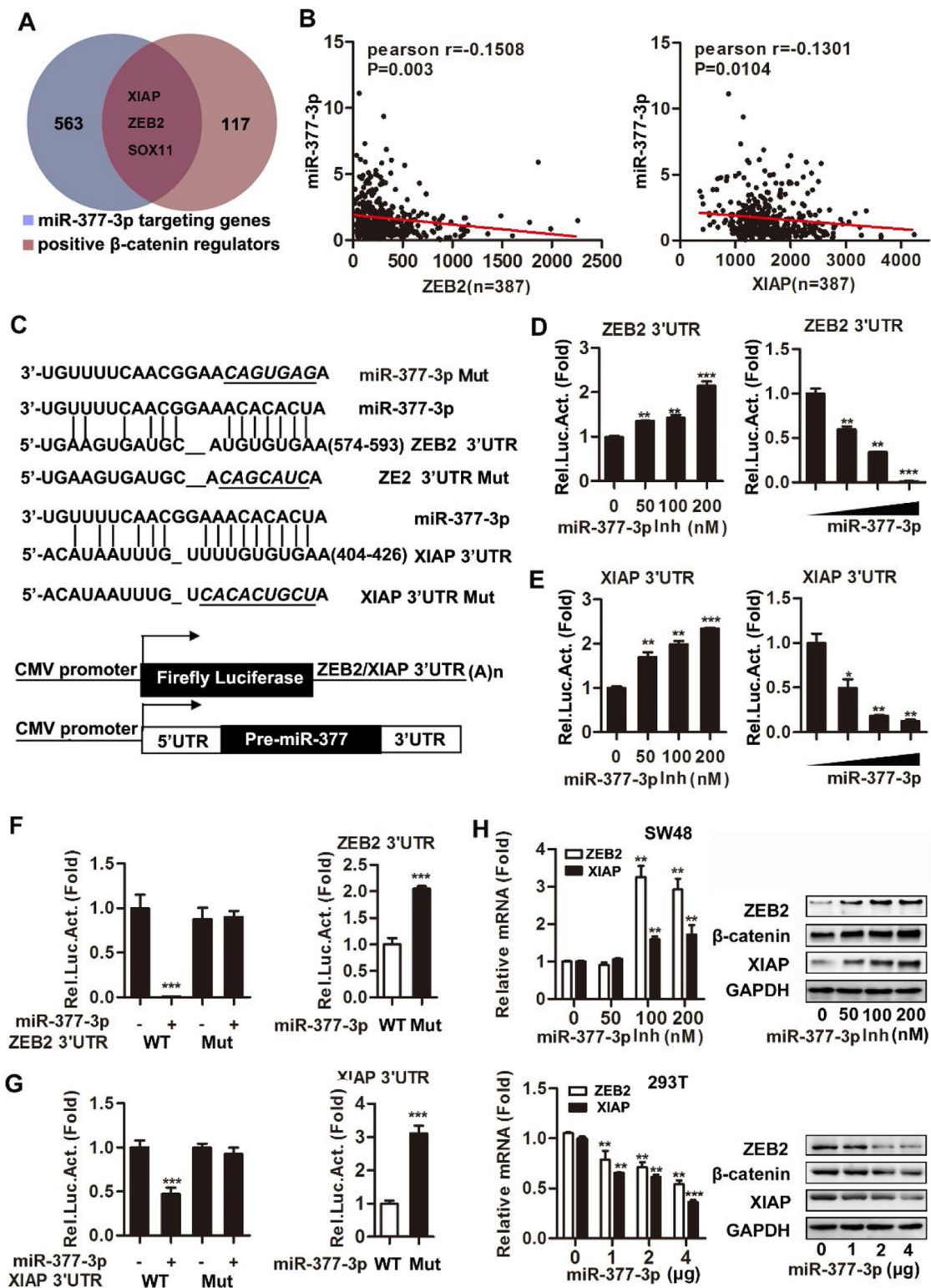


Fig. 4. ZEB2 and XIAP are the target genes of miR-377-3p. (A) Overlap of miR-377-3p target genes predicted by *TargetSan* and the genes positively regulating β -catenin from *NCBI-AmiGO2*. (B) Pearson correlation analysis of miR-377-3p with ZEB2 or XIAP expression in CRC from TCGA. (C) Predicted miR-377-3p binding sites underlined in the 3'UTR of ZEB2 or XIAP. Perfect matches in seed regions were indicated by lines. Mutants (underlined) of the binding sites in ZEB2/XIAP-3'UTR and miR-377-3p were generated. (D and E) 293 T cells were co-transfected with miR-377-3p mimic or miR-377-3p inhibitor and the wild-type 3'UTR of ZEB2 (D) or XIAP (E) firefly luciferase reporter plasmid for 48 h. Luciferase activities were measured and normalized to Rellina luciferase. n = 3 samples per group; *, P < 0.05; **, P < 0.01; ***, P < 0.001. (F-G) 293 T cells were co-transfected with miR-377-3p mimic and the mutant 3'UTR of ZEB2 (F) or XIAP (G) firefly luciferase reporter plasmid for 48 h. Luciferase activity was measured and normalized to Rellina luciferase activity. n = 3 samples per group; ***, P < 0.001. (H) The miR-377-3p plasmid was transfected into 293 T cells at different doses (0, 1, 2, 4 μ g) or miR-377-3p inhibitor (miR-377-3p Inh) was transfected into SW48 cells at different concentrations (0, 50, 100, 200 nM) for 48 h. The expression of ZEB2 and XIAP was detected by western blot and qPCR.

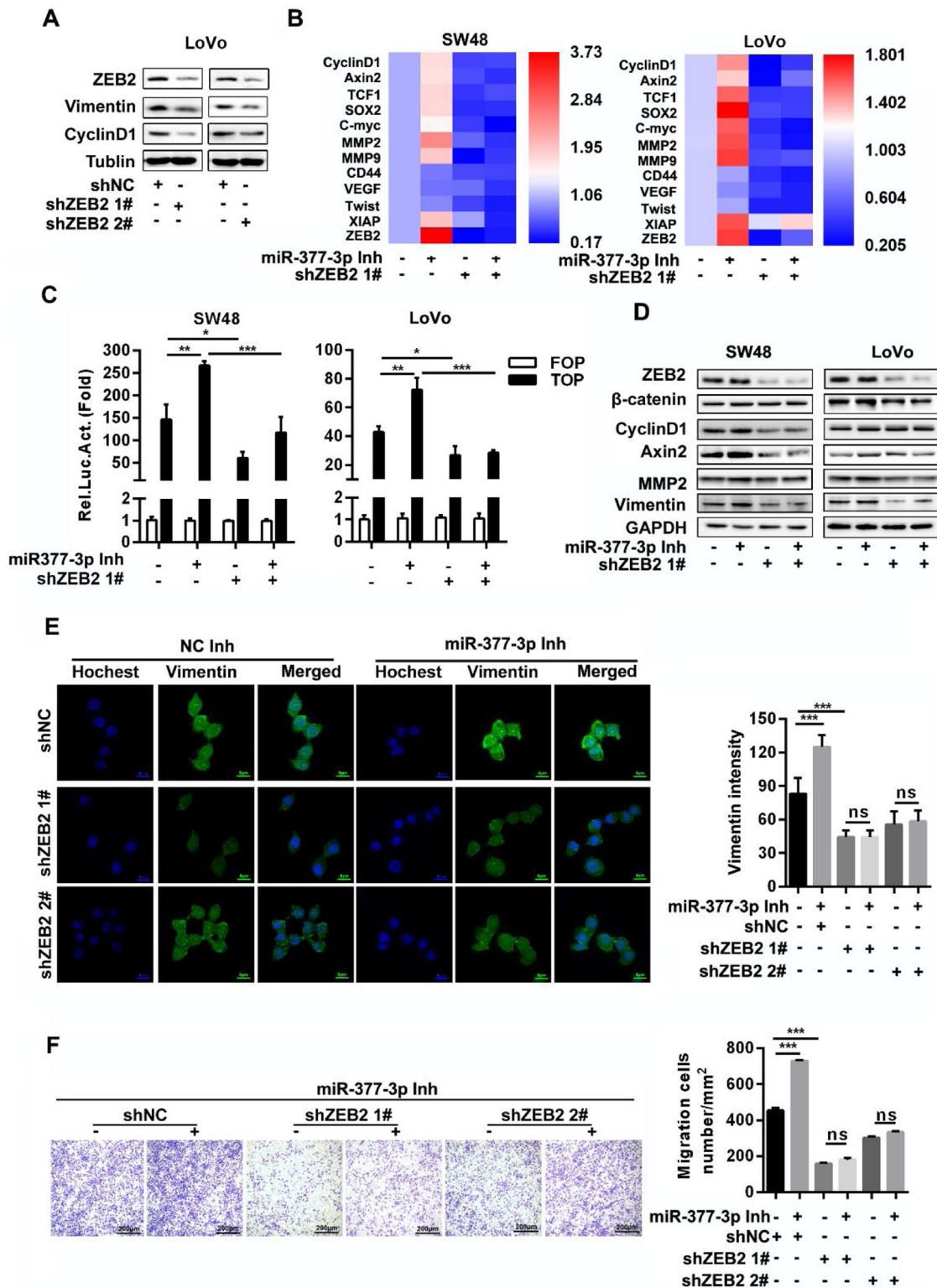


Fig. 5. MiR-377-3p inhibits CRC cell migration by targeting ZEB2. (A) The expression of Vimentin and CyclinD1 in ZEB2 stably knockdown LoVo cells was detected by western blot. (B) ZEB2 stably knockdown SW48 and LoVo cells were transfected with miR-377-3p inhibitor for 48 h. The downstream genes of Wnt signaling were detected by qPCR. The heatmap showed the changes in mRNA expression for the downstream genes of Wnt signaling. (C) ZEB2 stably knockdown SW48 and LoVo cells were co-transfected with miR-377-3p inhibitor and TOP-flash luciferase reporter for 48 h. Luciferase activity was measured and normalized to Rellina luciferase activity. $n = 3$ samples per group; *, $P < 0.05$; **, $P < 0.01$; ***, $P < 0.001$. (D) ZEB2 stably knockdown LoVo cells were transfected with miR-377-3p inhibitor for 48 h. ZEB2, β -catenin, Axin2, MMP2, Vimentin, CyclinD1 proteins were detected by western blot. (E) ZEB2 stably knockdown LoVo cells were transfected with miR-377-3p inhibitor for 48 h. Cells were fixed and stained for Vimentin. Representative images were shown and the fluorescence intensity was calculated. Scale bars, 8 μ m; ***, $P < 0.001$. (F) Migration assays of ZEB2 stably knockdown LoVo cells transfected with miR-377-3p inhibitor. Representative images were shown and the average number of cells per field were calculated. $n = 3$ samples per group, four fields per sample; Scale bars, 100 μ m; ***, $P < 0.001$; ns, no statistical significance.

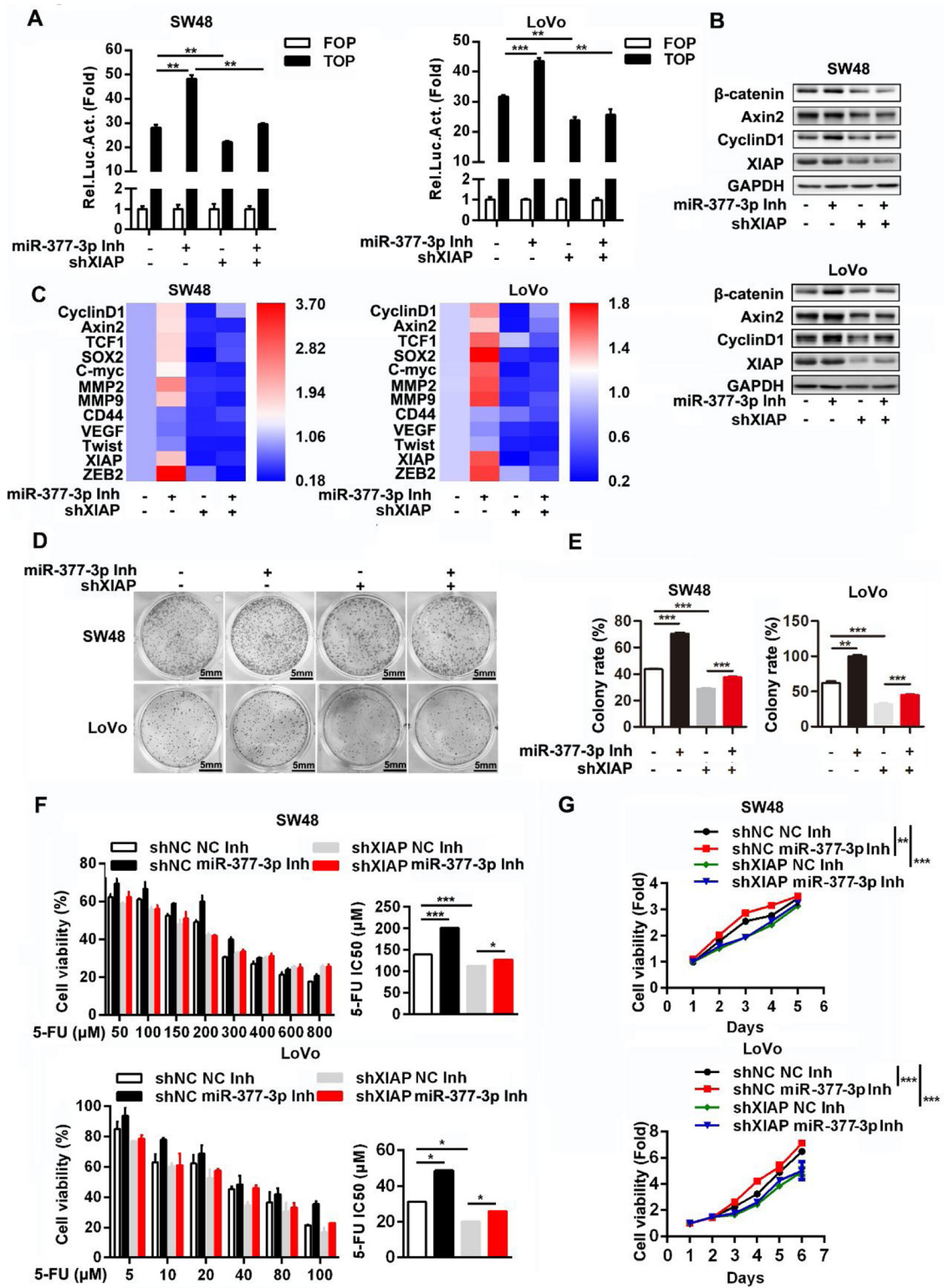


Fig. 6. MiR-377-3p suppresses CRC cell proliferation and chemoresistance via targeting XIAP. (A) XIAP stably knockdown SW48 and LoVo cells were co-transfected with miR-377-3p inhibitor and TOP-flash luciferase reporter for 48 h. Luciferase activity was measured and normalized to Renilla luciferase activity. n = 3 samples per group; **, P < 0.01; ***, P < 0.001. (B) XIAP stably knockdown LoVo cells were transfected with miR-377-3p inhibitor for 48 h. β-catenin, Axin2, CyclinD1 and XIAP proteins were detected by western blot. (C) XIAP stably knockdown SW48 and LoVo cells were transfected with miR-377-3p inhibitor for 48 h. The downstream genes of Wnt signaling were detected by qPCR. The heatmap showed the changes in mRNA expression for the downstream genes of Wnt signaling. (D and E) Colony formation assays of XIAP stably knockdown SW48 and LoVo cells transfected with miR-377-3p inhibitor (D) Colony numbers were calculated by ImageJ pro-plus (E). n = 3 samples per group; Scale bars, 5 mm; **, P < 0.01; ***, P < 0.001. (F) 5-FU cytotoxicity assays of XIAP stably knockdown SW48 and LoVo cells transfected with miR-377-3p inhibitor. n = 3 samples per group; *, P < 0.05. **, P < 0.01. ***, P < 0.001. (G) Proliferation assays of XIAP stably knockdown SW48 and LoVo cells transfected with miR-377-3p inhibitor. n = 3 samples per group; **, P < 0.01; ***, P < 0.001.

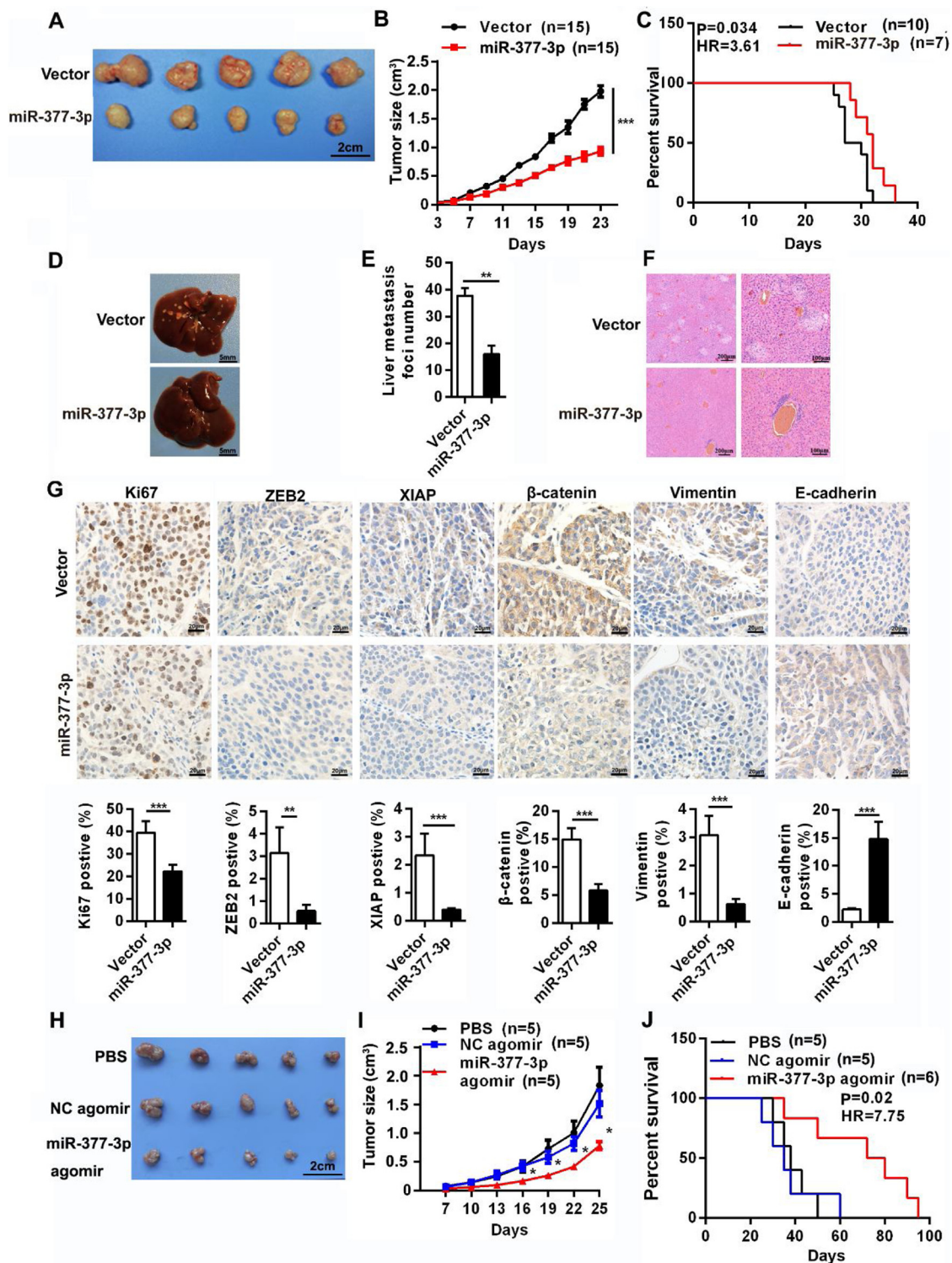


Fig. 7. MiR-377-3p inhibits CRC development and metastasis *in vivo*. (A and B) LoVo cells expressing Vector or miR-377-3p were subcutaneously injected into nude mice at a dose of 1×10^6 cells per mouse ($n = 15$ per group). Tumors isolated from the mice at day 23 post inoculation (A) and tumor growth curves (B) were shown. Scale bars, 2 cm; ***, $P < 0.001$. (C) Kaplan-Meier survival analysis of the two groups ($n = 10$ per group). (D and E) The representative images (D) of livers isolated from the nude mice described in (A) and the number of liver metastatic foci were counted (E). Scale bars, 5 mm; **, $P < 0.01$. (F) The representative HE staining of the livers isolated from the nude mice described in (A). Scale bars, 200 μ m. (G) Immunohistochemical staining of Ki67, ZEB2, XIAP, β -catenin, Vimentin, E-cadherin in tumors isolated from the nude mice described in (A). The representative images (upper panel) and the statistical proportions of positive cells (lower panel) are shown. Scale bars, 20 μ m; **, $P < 0.01$; ***, $P < 0.001$. (H–I) 1×10^6 LoVo cells were subcutaneously inoculated into nude mice ($n = 5$ per group). Once the tumors reached 0.5 cm³, the mice were randomized to receive the treatments of PBS, miR-377-3p agomir (75 mg/kg) or NC agomir (75 mg/kg) every 3 days for consecutive 6 times. Eighteen days after the treatment, the mice were euthanized and the tumors were isolated. Isolated tumors (H) and tumor growth curves (I) were shown. Scale bars, 2 cm; *, $P < 0.05$. (J) Kaplan-Meier survival analysis of the three treatment groups described in (H).

Major Human Diseases Program (2017) of Tongji Medical College, Huazhong University of Science and Technology; the Academic Medical Doctor Program (2018) of Tongji Medical College, Huazhong University of Science and Technology.

Appendix A. Supplementary data

Supplementary material related to this article can be found, in the online version, at doi:<https://doi.org/10.1016/j.phrs.2020.104774>.

References

- [1] F. Bray, J. Ferlay, I. Soerjomataram, R.L. Siegel, L.A. Torre, A. Jemal, Global cancer statistics 2018: GLOBOCAN estimates of incidence and mortality worldwide for 36 cancers in 185 countries, *CA Cancer J. Clin.* 68 (2018) 394–424.
- [2] E.P. Misiakos, N.P. Karidis, G. Kouraklis, Current treatment for colorectal liver metastases, *World J. Gastroenterol.* 17 (2011) 4067–4075.
- [3] A. Silvestri, E. Pin, A. Huijbers, R. Pellicani, E.M. Parasido, M. Pierobon, et al., Individualized therapy for metastatic colorectal cancer, *J. Intern. Med.* 274 (2013) 1–24.
- [4] H. Brenner, M. Kloor, C.P. Pox, Colorectal cancer, *Lancet* 383 (2014) 1490–1502.
- [5] P. Huang, R. Yan, X. Zhang, L. Wang, X. Ke, Y. Qu, Activating Wnt/beta-catenin signaling pathway for disease therapy: challenges and opportunities, *Pharmacol. Ther.* (2018).
- [6] H. Clevers, Wnt/beta-catenin signaling in development and disease, *Cell* 127 (2006) 469–480.
- [7] B.D. White, A.J. Chien, D.W. Dawson, Dysregulation of Wnt/beta-catenin signaling in gastrointestinal cancers, *Gastroenterology* 142 (2012) 219–232.
- [8] X. Cheng, X. Xu, D. Chen, F. Zhao, W. Wang, Therapeutic potential of targeting the Wnt/beta-catenin signaling pathway in colorectal cancer, *Biomed. Pharmacother.* 110 (2019) 473–481.
- [9] H. Clevers, R. Nusse, Wnt/beta-catenin signaling and disease, *Cell* 149 (2012) 1192–1205.
- [10] J. Behrens, J.P. von Kries, M. Kuhl, L. Bruhn, D. Wedlich, R. Grosschedl, et al., Functional interaction of beta-catenin with the transcription factor LEF-1, *Nature* 382 (1996) 638–642.
- [11] C. Lv, F. Li, X. Li, Y. Tian, Y. Zhang, X. Sheng, et al., MiR-31 promotes mammary stem cell expansion and breast tumorigenesis by suppressing Wnt signaling antagonists, *Nat. Commun.* 8 (2017) 1036.
- [12] S. Chai, K.Y. Ng, M. Tong, E.Y. Lau, T.K. Lee, K.W. Chan, et al., Octamer 4/ microRNA-1246 signaling axis drives Wnt/beta-catenin activation in liver cancer stem cells, *Hepatology* 64 (2016) 2062–2076.
- [13] L. Ren, H. Chen, J. Song, X. Chen, C. Lin, X. Zhang, et al., MiR-454-3p-Mediated Wnt/beta-catenin signaling antagonists suppression promotes breast Cancer metastasis, *Theranostics* 9 (2019) 449–465.
- [14] A. Lujambio, S.W. Lowe, The microcosmos of cancer, *Nature* 482 (2012) 347–355.
- [15] G. Di Leva, M. Garofalo, C.M. Croce, MicroRNAs in cancer, *Annu. Rev. Pathol.* 9 (2014) 287–314.
- [16] S. Giordano, A. Columbano, MicroRNAs: new tools for diagnosis, prognosis, and therapy in hepatocellular carcinoma? *Hepatology* 57 (2013) 840–847.
- [17] R. Zhang, H. Luo, S. Wang, W. Chen, Z. Chen, H.W. Wang, et al., MicroRNA-377 inhibited proliferation and invasion of human glioblastoma cells by directly targeting specificity protein 1, *Neuro Oncol* 16 (2014) 1510–1522.
- [18] B. Li, W.W. Xu, L. Han, K.T. Chan, S.W. Tsao, N.P.Y. Lee, et al., MicroRNA-377 suppresses initiation and progression of esophageal cancer by inhibiting CD133 and VEGF, *Oncogene* 36 (2017) 3986–4000.
- [19] H. Wu, H.Y. Liu, W.J. Liu, Y.L. Shi, D. Bao, miR-377-5p inhibits lung cancer cell proliferation, invasion, and cell cycle progression by targeting AKT1 signaling, *J. Cell. Biochem.* (2018).
- [20] C.Q. Wang, L. Chen, C.L. Dong, Y. Song, Z.P. Shen, W.M. Shen, et al., MiR-377 suppresses cell proliferation and metastasis in gastric cancer via repressing the expression of VEGFA, *Eur. Rev. Med. Pharmacol. Sci.* 21 (2017) 5101–5111.
- [21] S.M. Hammond, An overview of microRNAs, *Adv. Drug Deliv. Rev.* 87 (2015) 3–14.
- [22] C.W. Wu, S.S. Ng, Y.J. Dong, S.C. Ng, W.W. Leung, C.W. Lee, et al., Detection of miR-92a and miR-21 in stool samples as potential screening biomarkers for colorectal cancer and polyps, *Gut* 61 (2012) 739–745.
- [23] K. Hur, Y. Toiyama, Y. Okugawa, S. Ide, H. Imaoka, C.R. Boland, et al., Circulating microRNA-203 predicts prognosis and metastasis in human colorectal cancer, *Gut* 66 (2017) 654–665.
- [24] S. Qi, Y. Song, Y. Peng, H. Wang, H. Long, X. Yu, et al., ZEB2 mediates multiple pathways regulating cell proliferation, migration, invasion, and apoptosis in glioma, *PLoS One* 7 (2012) e38842.
- [25] C. Vandewalle, J. Comijn, B. De Craene, P. Vermassen, E. Bruyneel, H. Andersen, et al., SIP1/ZEB2 induces EMT by repressing genes of different epithelial cell-cell junctions, *Nucleic Acids Res.* 33 (2005) 6566–6578.
- [26] A.J. Hanson, H.A. Wallace, T.J. Freeman, R.D. Beauchamp, L.A. Lee, E. Lee, XIAP monoubiquitylates Groucho/TLE to promote canonical Wnt signaling, *Mol. Cell* 45 (2012) 619–628.
- [27] K. Connolly, R. Mitter, M. Muir, D. Jodrell, S. Guichard, Stable XIAP knockdown clones of HCT116 colon cancer cells are more sensitive to TRAIL, taxanes and irradiation in vitro, *Cancer Chemother. Pharmacol.* 64 (2009) 307–316.
- [28] R. Garzon, G. Marcucci, C.M. Croce, Targeting microRNAs in cancer: rationale, strategies and challenges, *Nat. Rev. Drug Discov.* 9 (2010) 775–789.
- [29] G. Chen, L. Lu, C. Liu, L. Shan, D. Yuan, MicroRNA-377 suppresses cell proliferation and invasion by inhibiting TIAM1 expression in hepatocellular carcinoma, *PLoS One* 10 (2015) e0117714.
- [30] X.G. Liu, J. Xu, F. Li, M.J. Li, T. Hu, Down-regulation of miR-377 contributes to cisplatin resistance by targeting XIAP in osteosarcoma, *Eur. Rev. Med. Pharmacol. Sci.* 22 (2018) 1249–1257.
- [31] C. Ye, Y. Hu, J. Wang, MicroRNA-377 targets zinc finger E-box-Binding homeobox 2 to inhibit cell proliferation and invasion of cervical Cancer, *Oncol. Res.* 27 (2019) 183–192.
- [32] W.Y. Liu, Z. Yang, Q. Sun, X. Yang, Y. Hu, H. Xie, et al., miR-377-3p drives malignancy characteristics via upregulating GSK-3beta expression and activating NF-kappaB pathway in hCRC cells, *J. Cell. Biochem.* 119 (2018) 2124–2134.
- [33] M. Bienz, H. Clevers, Linking colorectal cancer to Wnt signaling, *Cell* 103 (2000) 311–320.
- [34] R. Nusse, H. Clevers, Wnt/beta-catenin signaling, disease, and emerging therapeutic modalities, *Cell* 169 (2017) 985–999.
- [35] E.M. Schatoff, B.I. Leach, L.E. Dow, Wnt signaling and colorectal Cancer, *Curr. Colorectal Cancer Rep.* 13 (2017) 101–110.
- [36] R. Rupaimoole, F.J. Slack, MicroRNA therapeutics: towards a new era for the management of cancer and other diseases, *Nat. Rev. Drug Discov.* 16 (2017) 203–222.
- [37] D.L. Chen, Y.X. Lu, J.X. Zhang, X.L. Wei, F. Wang, Z.L. Zeng, et al., Long non-coding RNA UICLM promotes colorectal cancer liver metastasis by acting as a ceRNA for microRNA-215 to regulate ZEB2 expression, *Theranostics* 7 (2017) 4836–4849.
- [38] Y.B. Zheng, H.P. Luo, Q. Shi, Z.N. Hao, Y. Ding, Q.S. Wang, et al., miR-132 inhibits colorectal cancer invasion and metastasis via directly targeting ZEB2, *World J. Gastroenterol.* 20 (2014) 6515–6522.
- [39] G. Xiang, X. Wen, H. Wang, K. Chen, H. Liu, Expression of X-linked inhibitor of apoptosis protein in human colorectal cancer and its correlation with prognosis, *J. Surg. Oncol.* 100 (2009) 708–712.